Mineralogical Magazine, February 1999, Vol. 63(1), pp. 75–83

Synthesis of thallium-leucite ($TlAlSi_2O_6$) pseudomorph after analcime

A. KYONO, M. KIMATA, M. SHIMIZU

Institute of Geoscience, University of Tsukuba, 1-1-1 Tennodai, Tsukuba, Ibaraki 305-8571, Japan

S. SAITO

Institute of Materials Science, University of Tsukuba, 1-1-1 Tennodai, Tsukuba, Ibaraki 305-8573, Japan

N. NISHIDA

Chemical Analysis Center, University of Tsukuba, 1-1-1 Tennodai, Tsukuba, Ibaraki 305-8577, Japan

AND

T. HATTA

Japan International Research Center for Agricultural Sciences, Ministry of Agriculture, Forestry and Fisheries, 1–2 Ohwashi, Tsukuba, Ibaraki 305-8686, Japan

ABSTRACT

Thallium leucite, $TlAlSi_2O_6$, has been synthesized at 450°C for 7 days, under ambient conditions, by the transformation of dehydrated analcime $NaAlSi_2O_6$ in the presence of excess TlCl. This substitution of Tl for Na leads to confirmation of a thallium-leucite pseudomorph after analcime. Their optical properties, X-ray powder diffraction patterns, electron microprobe analysis, infrared spectra, and X-ray photoelectron spectroscopy have characterized the synthetic Tl-leucites. The IR spectra show that the mid-IR modes *T*-O stretching and *T*-O-*T* bending vibrations for $TlAlSi_2O_6$ are more resemblant of those for analcime than for leucite, $KAlSi_2O_6$. This resemblance implies that Tl cation enters the *W*-site rather than the *S*-site in the analcime structure: Na (*S*) + H_2O (*W*) $\rightleftharpoons$ □ + K (leucite) $\rightleftharpoons$ □ + Tl (Tl-leucite), where □ represents an *S*-site vacancy. The mechanism of this substitution is supported by the crystal chemical constraints: inasmuch as the *S*-site is smaller than the *W*-site, Tl^+ cations being larger than Na^+ plainly prefer the latter site to the former. One inference from the binding energy for Tl^+ by XPS is that Tl^+ occupies the extra-framework site in synthetic leucite pseudomorph, rather than the smaller tetrahedral site. The difference in Al/Si disordering between analcime and leucite and the nonstoichiometry due to the solid solution of the $□Si_3O_6$ component into the leucite structure may provide a fundamental insight into understanding why $TlAlSi_2O_6$ deviates from the trend defined by K-, Rb- and $CsAlSi_2O_6$ leucite series on the *a*-*c* parameter diagram, inasmuch as these three cations in the leucite structure occupy the *W*-sites. Finally, synthesis of $TlAlSi_2O_6$ leucite has an implication for the existence of other polymorphs due to different degrees of Al/Si disordering, except for high- and low-temperature leucites already known: natural leucites crystallized directly through igneous processes are different from those formed by substitution of K for Na in analcimes.

KEYWORDS: thallium, leucite, pseudomorph, analcime, substitution.

Introduction

SYNTHETIC leucites have been investigated for petrological reasons (Mitchell, 1996) as well as for their interesting properties of technological importance as solid state ionic conductors (e.g. Palmer and Salje, 1990). The geochemical affinity between thallium (Tl) and potassium (K), which

results from the practically identical effective ionic radii, is responsible for the abundance of thallium in rock-forming minerals (Zemann, 1993; Černý *et al.*, 1985). Significant substitutions have been reported in particular for sulphates (e.g. dorallcharite; Zunic *et al.*, 1994) and silicates (perlialite; Artioli and Kvick, 1990). The detailed EMPA for some ammonioleucites discovered as a pseudomorph after analcime (Hori *et al.*, 1986) revealed the presence of thallium (Tl_2O, max. about 6.0%) inherent in the former mineral (Nishida *et al.*, 1997). Hydrothermal synthesis of Tl-leucite from analcime by ion exchange (Barrer and Hinds, 1953; Barrer *et al.*, 1953*a,b*) has yet to be confirmed, for example by successful indexing of X-ray diffraction patterns. Recent synthesis of the zeolite containing Tl showed that the thallium ion has a strong preference for the cancrinite cage (Norby *et al.*, 1991). In this paper $TlAlSi_2O_6$ crystals, synthesized by ion exchange as a pseudomorph after analcime at 450°C, were analysed with X-ray diffractometry (XRD), scanning electron microscopy (SEM), infrared spectrophotometry (FTIR) and X-ray photoelectron spectroscopy (XPS).

Experimental methods and results

Attempts at synthesizing Tl-leucite, $TlAlSi_2O_6$, have succeeded by the exchange reaction: $NaAlSi_2O_6{\cdot}H_2O$ (analcime) + $TlCl \rightarrow TlAlSi_2O_6 + NaCl + H_2O$. Analcime from Croft, Leicestershre, England, was selected as the precusor to Tl-leucite, because the dehydrated phase produced after heating the former at 355°C is apparently isotypic with leucite (Mazzi and Galli, 1978). The starting grains of analcime, selected to be <1 mm in diameter, were dehydrated by heating at 500°C for 6 h. Afterwards, a mixture of the dehydrated phase of analcime and TlCl (Na:Tl = 1:20) was inserted into an evacuated silica tube and then sealed by welding. The silica tube was heated at 450°C for each of two run times, 2 h and 7 days. Examination by EPMA and X-ray powder diffraction analysis revealed that the dehydrated analcime heated for 7 days had completely transformed into Tl-leucite, on which the description has been based below.

Scanning electron (SEM) micrographs show that crystals of synthetic Tl-leucite have the same morphology as the precursor analcime, as represented in Fig. 1. The Tl-leucite can, therefore, form as a pseudomorph after analcime. This relationship is consistent with the morphologies of ammonioleucite (Hori *et al.*, 1986) and Tl-bearing ammonioleucite (Nishida *et al.*, 1997), which occur as a pseudomorph after analcime. The sum image in backscattering energy, however, emphasizes compositional differences

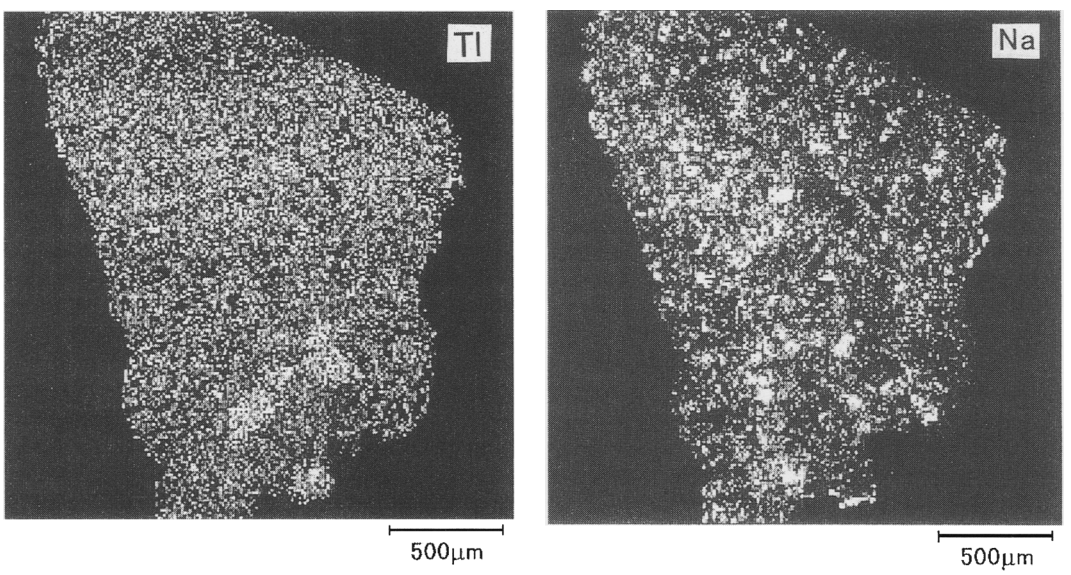

FIG. 1. Back-scattered electron images of Tl-leucite synthesized from analcime at 450°C for 2 h; light tones indicate increased contents of Tl and Na cations.

between Tl-leucite and analcime. In spite of invariation in morphology of analcime, substitution of Tl for Na + H_2O gives rise to the formation of Tl-leucite (Fig. 1).

The powdered sample was mounted on a non-reflecting quartz plate; the X-ray powder (XRD) patterns were collected on a Rigaku X-ray diffractometer and studied with Cu-$K\alpha_1$ radiation, λ = 1.54056 Å. The d_{hkl}-I_{hkl} listings are tabulated in Table 1. Line indexing and identification for Tl-leucite were based on Powder Diffraction System file 40-474 for ammonioleucite (Hori *et al.*, 1986) and for Tl-bearing ammonioleucite (Nishida *et al.*, 1997). The general agreement between Tl-analcime (Barrer *et al.*, 1953) and the other leucites is good. Least-squares fitting of the *d* values (Holland and Redfern, 1997) gave cell dimensions a = 13.269 (2), c = 13.718 (2) Å, and V = 2415.1(9) Å^3 for synthetic Tl-leucite, in contrast with those of the present analcime with cubic symmetry: a = 13.7104(9) Å and V = 2577.2(5) Å^3. The refined cell parameters of this Tl-leucite are larger than those for ammonioleucite (a = 13.214(1), c = 13.713(2) Å and V = 2394.4 Å^3; Hori *et al.*, 1986) and for Tl-bearing ammonioleucite (a = 13.237(3), c = 13.724(5) Å and V = 2404.7 Å^3; Nishida *et al.*, 1997). This probably reflects the differences in ionic radii among Tl^+, NH_4^+ and K^+ (Shannon, 1976) occupying the extra-framework sites in these leucites.

Electron microprobe analyses (EPMA) were made using a JEOL superprobe operating in the wavelength-dispersive mode at 20 kV and 10 nA. The standards used were lorandite for Tl, corundum for Al, quartz for Si, albite for Na and microcline for K. The chemical composition of the synthetic Tl-leucite calculated from the data averaged over six electron-probe analyses is $(Tl_{0.929}Al_{0.021}\square_{0.050})Al_{0.992}Si_{2.008}O_6$ (Table 2). Excess silica in Tl-leucite merits general recognition by mineralogists interested in framework silicates (e.g. Grundy and Ito, 1974; Kimata, 1988; Smith and Brown, 1988; Kimata *et al.*, 1995).

The FTIR spectra of leucite groups, recorded over the mid-infrared region in powder absorption mode using the KBr pellet method, are given in Fig. 2. The overall IR spectrum of Tl-leucite resembles that of natural analcime rather than of natural leucite. This general resemblance in the region of (Al,Si)-O stretching vibrations indicates that the Al/Si disordering at the tetrahedral framework-sites of synthetic Tl-leucite is the same as that in natural analcime, differing from the Al/Si distribution of natural leucite. It is quite within reason, however, that the differences in the reduced mass and force constant between Tl and K causes all peaks to be slightly shifted below 1000 cm^{-1} toward the lower wavenumber side, as compared with those for natural leucite.

X-ray photoelectron spectroscopy (XPS) provides scope for additional interpretation of the oxidation and structural state of target atoms (Hochella, 1995). After careful calibration and standardization of our XPS instrument, SIENTA ESCA-300, the Tl *4f* spin-orbit split photopeak pairs are measured for synthetic Tl-leucite, Tl_2O_3 and TlCl as shown in Fig. 3. Each binding energy for Tl $4f_{5/2}$ and Tl $4f_{7/2}$ clearly indicates that the binding energy for Tl in Tl-leucite is closer to that in Tl_2O_3 rather than in TlCl. One inference from this similarity is that thallium in the synthetic leucite pseudomorph has been detected as Tl cations in oxides, rather than those in chlorides of the starting material. There have been no reliable XPS data concerning the difference in binding energy between Tl^+ and Tl^{3+} in silicates.

Discussion

Crystal chemistry of Tl-leucite

A plot of the *a*, *c*-lattice constants of some leucite-type compounds is represented in Fig. 4.

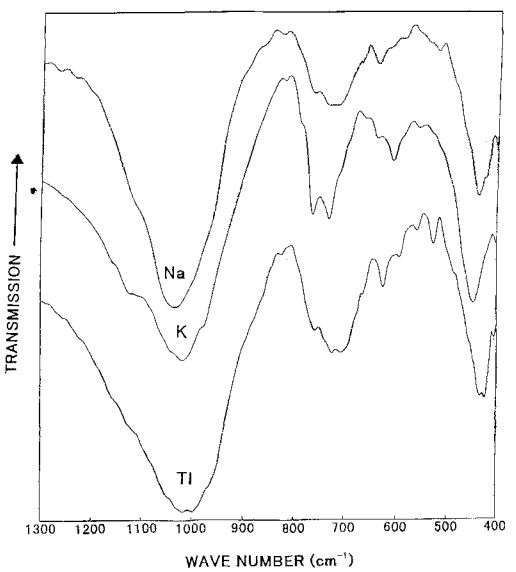

FIG. 2. Infrared absorption spectra of leucite, Tl-leucite and analcime.

TABLE 1. Powder X-ray diffraction data for Tl-leucites and ammonioleucite

	Synthetic Tl-leucite			Tl-analcime[1]		Tl-bearing NH_4-leucite[2]		NH_4-leucite[3]	
h k l	d_{obs}(Å)	d_{calc}(Å)	d/d_0	*d*(Å)	I/I_0	*d*(Å)	I/I_0	*d*(Å)	I/I_0
1 0 1	9.50	9.50	<2			9.53	11	9.50	3
2 0 0	6.64	6.63	2			6.60	7	6.59	2
1 1 2	5.53	5.54	14	5.54	80	5.54	38	5.53	50
2 1 1	5.45	5.45	18			5.44	81	5.43	100
2 0 2	4.77	4.77	2			4.76	8	4.75	5
2 1 3	3.62	3.62	28	3.60	100	3.61	5	3.61	1
3 2 1	3.56	3.55	24			3.54	12	3.54	7
0 0 4	3.43	3.43	70			3.43	55	3.43	40
4 0 0	3.32	3.32	100	3.35	100	3.31	100	3.30	80
3 0 3	3.18	3.18	2			3.18	5	3.17	2
4 1 1	3.13	3.13	10			3.13	7	3.12	3
2 0 4	3.04	3.05	2			3.04	6	3.04	3
4 2 0	2.969	2.967	10	2.98	20	2.960	17	2.955	20
3 2 3	2.868	2.867	34	2.87	80	2.862	17	2.859	20
3 3 2	2.847	2.846	14			2.860	16	2.839	10
4 2 2	2.722	2.723	2			2.718	4	2.714	1
3 1 4	2.655	2.655	4	2.651	20	2.656	7	2.653	7
4 1 3	2.634	2.632	2			2.625	5	2.624	2
2 1 5	2.491	2.490	6			2.486	6	2.489	3
5 1 2	2.429	2.433	10	2.431	20	2.422	6	2.422	3
4 0 4	2.385	2.384	28	2.378	70	2.383	7	2.379	7
4 4 0	2.346	2.346	8			2.334	4	2.333	2
3 0 5	2.333	2.332	2						
4 3 3	2.297	2.295	2			2.290	4	2.288	1
1 1 6	2.222	2.221	4			2.218	3	2.218	1
3 2 5	2.200	2.200	8			2.197	3	2.197	1
5 3 2	2.160	2.160	12	2.163	70	2.152	5	2.153	5
6 2 0	2.090	2.098	<2			2.092	3	2.088	2
5 4 1	2.041	2.049	<2			2.039	3	2.042	1
6 2 2	2.007	2.006	4			2.006	3	1.999	1
				1.966	40				
4 4 4	1.934	1.936	6	1.933	40	1.932	3	1.932	2
5 4 3	1.883	1.888	<2			1.882	4	1.880	2
4 0 6	1.880	1.883	<2						
3 3 6	1.846	1.846	2			1.844	3	1.843	1
6 4 0	1.834	1.840	2			1.833	4	1.834	1
4 2 6	1.811	1.811	4			1.807	4	1.807	2
5 5 2	1.810	1.810	8	1.810	60				
7 0 3	1.752	1.751	2			1.746	3	1.745	1
3 2 7	1.731	1.730	4			1.729	3	1.729	2
5 1 6	1.715	1.718	4			1.715	3	1.715	1
0 0 8	1.714	1.715	4	1.712	40				
7 3 2	1.688	1.689	6	1.688	60	1.686	5	1.684	5
				1.662	20				
5 5 4	1.643	1.646	<2			1.643	3	1.641	1
				1.613	40				
8 2 0	1.609	1.609	2			1.605	4	1.604	2
6 5 3	1.594	1.593	2			1.588	3	1.588	1
3 1 8	1.589	1.587	2						
4 3 7	1.575	1.577	<2			1.576	2	1.574	1
				1.552	20				
7 4 3	1.545	1.549	<2			1.545	3	1.544	2

TABLE 1. (*contd.*)

	SynthenticTl-leucite			Tl-analcime[1]		Tl-bearing NH_4-leucite[2]		NH_4-leucite[3]	
h k l	d_{obs}(Å)	d_{calc}(Å)	d/d_0	*d*(Å)	I/I_0	*d*(Å)	I/I_0	*d*(Å)	I/I_0
6 2 6		1.546	<2						
				1.522	40				
7 5 2	1.505	1.505	<2			1.501	3	1.501	1
3 3 8		1.504	<2	1.497	40				
2 1 9	1.477	1.476	<2	1.457	10	1.476	3	1.476	1
9 1 2	1.433	1.433	2	1.433	10	1.427	3	1.427	1
7 6 1		1.431	2						
7 3 6	1.385	1.386	2	1.389	20	1.382	2	1.382	1
4 1 9	1.376	1.378	2			1.376	2	1.376	1
1 1 10	1.358	1.357	2	1.364	10	1.357	3	1.357	1
8 5 3	1.341	1.344	<2			1.336	3	1.337	1
8 0 6		1.343	<2						
8 6 0	1.323	1.327	<2			1.322	3	1.323	1
4 3 9	1.322	1.322	<2						
7 7 2	1.313	1.316	2			1.309	3	1.310	1
9 4 3	1.289	1.293	<2			1.290	3	1.288	1
6 6 6		1.291	<2						
9 5 2	1.266	1.267	2			1.262	3	1.262	1
6 1 9	1.249	1.249	<2			1.246	3	1.248	1
10 3 3	1.222	1.225	<2						
2 1 11	1.220	1.220	<2			1.220	3	1.220	1
8 3 7	1.215	1.217	<2			1.212	3	1.214	1

*d_{calc} based on refined cell parameters: synthetic Tl-leucite, a = 13.269(2), c = 13.718(2)Å.
[1] Barrer and Hinds (1950). [2] Nishida *et al.* (1997). [3] Hori *et al.* (1986).

Increasing the size of monovalent cations in non-tetrahedral sites of the leucite groups with the identical framework leads to the geometrical variation of their unit-cells expanding along the *a* axes and contracting along the *c* axes (Torres-Martinez and West, 1989). This variation in the substituted structures follows the idea of partial collapse in tetrahedral-framework structures proposed by Taylor and Henderson (1968). The mechanism of expansion in their unit-cells can be explained by variation in *T*-O-*T* angles: the cation radius increases from K^+ to Cs^+, and so the mean *T*-O-*T* angle of the leucite-type framework increases to 144.5° (Liebau, 1985). This increase in the mean *T*-O-*T* angles gives rise to expansion of the *a*-axes and contraction of *c*-axes in the leucite-type unit-cells.

Thallium (1.50 Å) is so similar in ionic radius to rubidium (1.52 Å) that the cell dimensions of $TlAlSi_2O_6$ and $RbAlSi_2O_6$ approximate to each other. Nevertheless the data for Tl-leucite plot off the curve connecting its K-, Rb- and Cs-type equivalents. The deviation is partly due to the solubility of excess silica as a $\square Si_3O_6$ component ($\square$ = extra-framework site vacancy) in the Tl-leucite, which contributes to the shrinkage of the extra-framework site linked with slight shortening of its cell parameters. This finding of non-stoichiometry from synthetic Tl-leucite is consistent with several observations on natural leucites (Gupta and Yagi, 1980).

Site-preference of Tl cation

The site-preference of thallium in the crystal structure of synthesized Tl-leucite remains a subject for considerable debate. Inasmuch as the ionic size of Tl^+ cannot satisfy crystal-chemical requirements for the tetrahedral framework-sites, attention is focused on discriminating the extra-framework sites favourable for large alkali cations.

Analcime, one of the zeolite groups, is a common framework silicate mineral having the chemical formula $NaAlSi_2O_6 \cdot H_2O$ and the space group $I4_1/acd$. This zeolite has a system of non-intersecting channels parallel to triple axes of a (pseudo) cubic lattice along [111] (Pechar, 1988). The cavities of the analcime-type framework

TABLE 2. Representative microprobe analyses of Tl-leucite and natural analcime

	$TlAlSi_2O_6$	Analcime	Tl-leucite	
	calc.	*obs.*	*obs.*	
SiO_2	31.33	58.67	32.76	
Al_2O_3	13.29	21.81	13.99	
Na_2O	–	12.36	–	
Tl_2O	55.38	–	53.63	
Total (wt.%)	100.00	92.84	100.38	
Cation/6.00 Oxygen	*calc.*	*obs.*	*obs.*	*calc.**
Si	2.000	2.096	2.008	2.005
Al	1.000	0.918	1.013	1.009
Na	–	0.855	–	–
Tl	1.000	–	0.929	0.929
Total	4.000	3.869	3.950	3.943

End-member indication of synthetic Tl-leucite

	$TlAlSi_2O_6$	Tl-leucite
	calc.	*obs.*
$TlAlSi_2O_6$	100.0	92.9
$\square Si_3O_6$**	0.0	5.0
$Al(Al_3)O_6$	0.0	2.1
Total (wt.%)	100.0	100.0

*Calculated on the basis of end-member
**Excess silica component; □ stands for a defect at *M* site

contain two kinds of sites: Na(*S*) and H_2O(*W*), and *W*-positions are situated in the non-intersected channels (Moroz *et al.*, 1998). One third of sodium sites are vacant and located around the water molecule position. The structure of dehydrated analcime still retains a system of non-intersecting channels parallel to triple axes of a (pseudo) cubic lattice (Bakakin *et al.*, 1994). On the other hand, in leucite-type structures, the extra-framework-sites equivalent to the *W*-site in analcime can typically contain large cations like K, Rb and Cs (Gottardi and Galli, 1985). An analogy in the Si-O stretching vibration region of IR spectra has been drawn between synthetic Tl-leucites and analcime, rather than natural leucite (Fig. 2). The framework structure for analcime is topologically equivalent to that for leucite, but both of them are different from each other in Al/Si ordering degree and their angular distortion (Table 3). Indeed, ^{29}Si magic-angle-spinning NMR spectroscopy could provide detailed information on this difference in Si-Al ordering (Murdoch *et al.*, 1988). The temperature causing the dehydration of analcime is too low to promote Al/Si disordering in the tetrahedral framework of analcime, and the substitution of Tl for Na at 450°C cannot induce more Al/Si disordering in the tetrahedral structure of the dehydrated analcime. The conclusive reason is that above 665°C leucite is cubic, and below this temperature leucite transforms to tetragonal symmetry (Palmer *et al.*, 1989). Therefore the transformation of analcime into synthetic Tl-leucite under ambient conditions can be brought about through the following process

Dehydration: $NaAlSi_2O_6H_2O \rightarrow NaAlSi_2O_6 + H_2O$ (1)

Substitution: $Na(S)\square(W)-AlSi_2O_6 + TlCl \rightarrow \square(S)Tl(W)-AlSi_2O_6 + NaCl$ (2)

where Tl^+ cations presumably prefer the *W*-site to the *S*-site which is suitable for Na^+ and too small for the former cation.

$$\square(S)Tl(W)-AlSi_2O_6 \rightarrow TlAlSi_2O_6 \quad (3)$$

where Tl^+ occupies the *W*-site.

Thus it is natural that in the Al/Si disordering the synthetic Tl-leucite should accord with natural

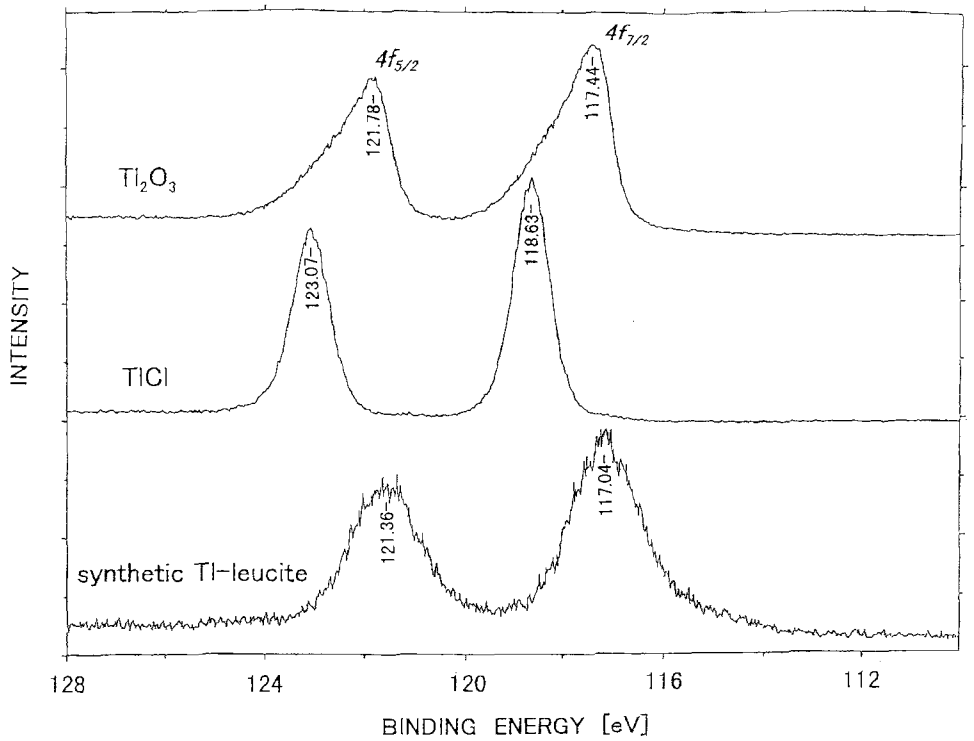

FIG. 3. Thallium *4f* XPS spectra of Tl-leucite, TlCl and Tl_2O_3 exposed on Al thin films. The main peak at lower binding energy is the Tl $4f_{7/2}$ line, while the higher binding energy peak is the Tl $4f_{5/2}$ line.

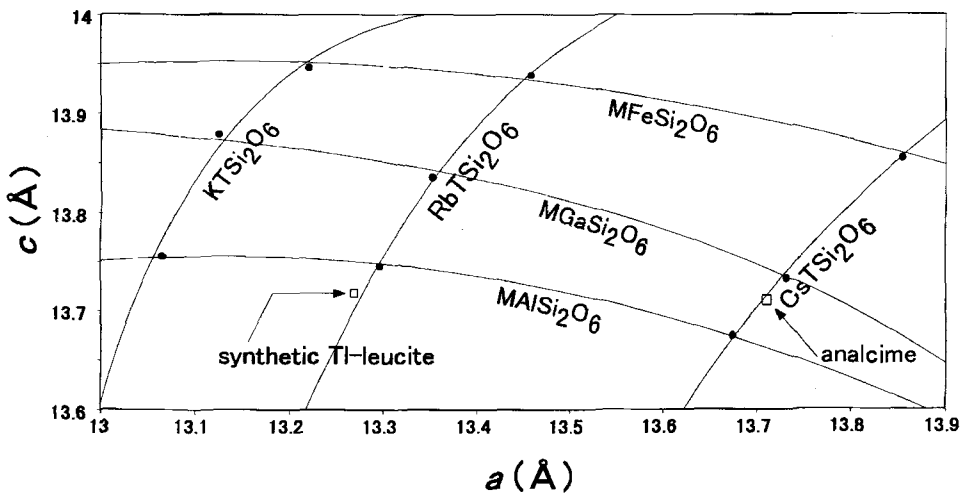

FIG. 4. Compilation of lattice parameters, *a vs. c* for leucite-type compounds. $KAlSi_2O_6$ (Wong-Ng *et al.*, 1987); $KGaSi_2O_6$ (Torres-Martinez and West, 1986); $KFeSi_2O_6$ (Bell and Henderson, 1994); $RbAlSi_2O_6$ (Martin and Lagache, 1987); $RbGaSi_2O_6$ (Torres-Martinez and West, 1986); $RbFeSi_2O_6$ (Bell and Henderson, 1994); $CsAlSi_2O_6$ (Newnham, 1967); $CsFeSi_2O_6$ (Bell and Henderson, 1994).

TABLE 3. Comparisons of mean *T*-O bond lengths, Al fraction, angular distortion and mean *T*-O-*T* angles between natural leucite and natural analcime

	Leucite			Analcime		
	T(1)	T(2)	T(3)	T(1)	T(2)	T(3)
Mean bond lengths (Å)	1.634	1.656	1.656	1.650	1.644	1.650
Al fraction: Al/(Si+Al)	0.25	0.32	0.32	0.35	0.30	0.35
Angular distortion	2.93	2.25	1.45	3.60	3.35	3.60
Mean *T*-O-*T* angles (°)		138.4				144.3

Leucite: Mazzi *et al.* (1976). Analcime: Mazzi and Gaili (1978)

analcime and differ from natural leucite. This accordance accounts for both the resemblance in the IR spectra between Tl-leucite and natural analcime and a unique contribution to the deviation of the former from the *a-c* curve connecting its K-, Rb- and Cs-type equivalents. The similarity in ionic radii between Tl^+ and Rb^+ also supports a partial occupation of *W*-sites by Tl cations. Therefore leucite may have more polymorphs due to different degrees of Al/Si disordering, except for high- and low-temperature leucites already well known (Palmer *et al.*, 1989). Their existence is evident from the detailed information on Si-Al ordering in leucites obtained with ^{29}Si MAS NMR (Murdoch *et al.*, 1988).

The earlier concept discussed by many authors (e.g. Ducros, 1960) that ion mobility decreases under dehydration of zeolites due to a stronger interaction of cations and framework oxygens has been repudiated by the present result: Tl cations rapidly transferring to the empty *W*-position in the dehydrated analcime. Furthermore it has been found that cation exchange, as well as dehydration, radically alter the dynamics of particles interposed in channels of the analcime framework (Moroz *et al.*, 1998). Their very existence is a challenge to our understanding of the ion-mobility rate depending on the crystal structure. Further studies on this topic, and particularly, concerning structural refinement for Tl-leucite in a single crystal are in progress.

Acknowledgements

Dr P. Berlepsch, Universitat Basel, Switzerland generously lent the lorandite synthesized for the standard of thallium by EPMA. We are greatly indebted to Prof. C.M.B. Henderson and Dr S.A.T. Redfern for their constructive reviews. Much appreciated technical assistance in the synthesis was provided by T. Matsui of the Department of Education, Kagoshima University.

References

Artioli, G. and Kvick, A. (1990) Synchrotron X-ray rietveld study of perlialite, the natural counterpart of synthetic zeolite-L. *Eur. J. Mineral.*, **2**, 749–759.

Bakakin, V.V., Alekseev, V.I., Seryotkin, Y.V., Belitsky, I.A. and Fursenko, B.A. (1994) Crystal structure of dehydrated analcime (in Russian). *Dokl. RAN.*, **339**, 520–4.

Barrer, R.M. and Hinds, L. (1950) Ion-exchange and ion-sieve processes in crystalline zeolites. *J. Chem. Soc.*, 2342–50.

Barrer, R.M. and Hinds, L. (1953) Ion-exchange in crystals of analcite and leucite. *J. Chem. Soc.*, 1879–88.

Barrer, R.M., Baynham, J.W. and McCallum, N. (1953*a*) Hydrothermal chemistry of the silicates. V. Compounds structurally related to analcite. *J. Chem. Soc.*, 4035–41.

Barrer, R.M., Hinds, L. and White, E.A. (1953*b*) The hydrothermal chemistry of silicates. Part III. Reactions of analcite and leucite. *J. Chem. Soc.*, 1466–75.

Bell, A.M.T. and Henderson, C.M.B. (1994) Rietveld refinement of the structures of dry-synthesized $M Fe^{III}Si_2O_6$ leucites (M = K, Rb, Cs) by synchrotron X-ray powder diffraction. *Acta Crystallogr.*, **C50**, 1531–6.

Černý, P., Meintzer, R.E. and Anderson, A.J. (1985) Extreme fractionation in rare-element granitic pegmatites: selected examples of data and mechanisms. *Canad. Mineral.*, **23**, 381–421.

Ducros, P. (1960) Etude de la mobilite de l'eau et des cations dans quelques zeolite par relaxation dielectrique et resonance magnetique nucleaire. *Bull. Soc. Fr. Mineral. Cristallogr.* **53**, 85–112.

Gottardi, G. and Galli, E. (1985) *Natural zeolites*. (Minerals and rocks, vol. **18**) Springer-Verlag, Berlin, Heidelberg, New York, 409 pp.

Grundy, H.D. and Ito, J. (1974) The refinement of the crystal structure of a synthetic non-stoichiometric Sr feldspar. *Amer. Mineral.*, **59**, 1319–26.

Gupta, A.K. and Yagi, K. (1980) *Petrology and Genesis of Leucite-Bearing Rocks*. Springer-Verlag, Berlin, 252 pp.

Hochella, M.F. Jr. (1995) Mineral surfaces: their characterization and their chemical, physical and reaction. In: *Mineral Surfaces*, (D.J. Vaughan and R.A.D. Pattrick, eds) Chapman & Hall, London, pp. 17–60.

Holland, T.J.B. and Redfern, S.A.T. (1997) Unit cell refinement from powder diffraction data: the use of regression diagnostics. *Mineral. Mag.*, **61**, 65–77.

Hori, H., Nagashima, K., Yamada, M., Miyawaki, R. and Marubashi, T. (1986) Ammonioleucite, a new mineral from Tatarazawa, Fujioka, Japan. *Amer. Mineral.*, **71**, 1022–7.

Kimata, M. (1988) The crystal structure of non-stoichiometric Eu-anorthite: an explanation of the Eu-positive anomaly. *Mineral. Mag.*, **52**, 257–65.

Kimata, M., Nishida, N., Shimizu, M., Saito, S., Matsui, T. and Arakawa, Y. (1995) Anorthite megacrysts from the island arc basalt. *Mineral. Mag.*, **59**, 1–14.

Liebau, F. (1985) *Structural Chemistry of Silicates*. Springer-Verlag, Berlin, 347 pp.

Martin, R.F. and Lagache, M. (1975) Cell edges and infrared spectra of synthetic leucites and pollucites in the system $KAlSi_2O_6$-$RbAlSi_2O_6$-$CsAlSi_2O_6$. *Canad. Mineral.*, **13**, 275–81.

Mazzi, F., Galli, E. and Gottardi, G. (1976) The crystal structure of tetragonal leucite. *Amer. Mineral.*, **61**, 108–15.

Mazzi, F. and Galli, E. (1978) Is each analcime different? *Amer. Mineral.*, **63**, 448–60.

Mitchell, R.H. (1996) *Undersaturated Alkaline Rocks: Mineralogy, Petrogenesis, and Economic Potential*. Short Course Vol. **24**, Miner. Assoc. Canada, 312 pp.

Moroz, N.K., Afanassyev, I.S., Fursenko, B.A. and Belitsky, I.A. (1998) Ion mobility and dynamic disordering of water in analcime. *Phys. Chem. Minerals*, **25**, 282–7.

Murdoch, J.B., Stebbins, J.F., Carmichael, I.S.E. and Pines, A. (1988) A silicon-29 nuclear magnetic resonance study of silicon-aluminum ordering in leucite and analcite. *Phys. Chem. Minerals*, **15**, 370–82.

Newnham, R.E. (1967) Crystal structure and optical properties of pollucite. *Amer. Mineral.*, **52**, 1515–8.

Nishida, N., Kimata, M., Kyono, A., Togawa, Y., Shimizu, M. and Hori, H. (1997) First finding of thallium-bearing ammonioleucite: A signal for the ultimate stage of the hydrothermal process and for a far-reaching effect from seawater alteration of MORB. *Ann. Rep., Inst. Geosci., Univ. Tsukuba*, **23**, 35–41.

Norby, P., Andersen, I.G. Krogh, Andersen, E. Krogh, Colella, C. and De'Gennaro, M. (1991) Synthesis and structure of lithium cesium and lithium thallium cancrinites. *Zeolites*, **11**, 248–53.

Palmer, D.C., Salje, E. and Schmahl, W.W. (1989) Phase transitions in leucite: X-ray diffraction studies. *Phys. Chem. Minerals*, **16**, 714–9.

Palmer, D.C. and Salje, E.K.H. (1990) Phase-transitions in leucite dielectric properties and transition mechanism. *Phys. Chem. Minerals.*, **17**, 444–52.

Pechar, F. (1988) The crystal structure of natural monoclinic analcime ($NaAlSi_2O_6.H_2O$). *Z. Kristallogr.*, **184**, 63–9.

Shannon, R.D. (1976) Revised effective ionic radii and systematic studies of interatomic distances in halides and chalcogenides. *Acta Crystallogr.*, **A32**, 751–68.

Smith, J.V. and Brown, W.L. (1988) *Feldspar Minerals, I. Crystal structure, Physical, Chemical, and Microtextural Properties*. Springer-Verlag, Berlin, 828 pp.

Taylor, D. and Henderson, C.M.B. (1968) The thermal expansion of the leucite group of minerals. *Amer. Mineral.*, **53**, 1476–89.

Torres-Martinez, L.M. and West, A.R. (1986) New family of phases with the pollucite structure. *Z. Kristallogr.*, **175**, 1–7.

Torres-Martinez, L.M. and West, A.R. (1989) Pollucite-related and leucite-related phases ($A_2BX_5O_{12}$ and ACX_2O_6; A – K, Rb, Cs; B – Be, Mg, Fe, Co, Ni, Cu, Zn, Cd; C – B, Al, Ga, Fe, Cr; X – Si, Ge). *Z. Anorg. Chem.*, **576**, 223–30.

Wong-Ng, W., McMurdie, F.H., Paretzkin, B., Hubbard, C.R., Dragoo, A.L. and Stewart, J.M. (1987) Standard X-ray diffraction powder patterns of fifteen ceramic phases. *Powder Diffraction*, **2(2)**, 106–17.

Zemann, J. (1993) Thallium in Mineralogie und Geochemie. *Mitt. Osterr. Mineral. Ges.*, **138**, 75–91.

Zunic, T.B., Moelo, Y., Loncar, Z. and Micheelsen, H. (1994) Dorallcharite, $Tl_{0.8}K_{0.2}Fe_3(SO_4)_2(OH)_6$, a new member of the jarosite-alunite family. *Eur. J. Mineral.*, **6**, 255–63.

[*Manuscript received 4 March 1998; revised 1 July 1998*]